RNAi living-cell microarrays for loss-of-function screens in *Drosophila melanogaster* cells

Douglas B Wheeler, Steve N Bailey, David A Guertin, Anne E Carpenter, Caitlin O Higgins & David M Sabatini

RNA interference (RNAi)-mediated loss-of-function screening in *Drosophila melanogaster* tissue culture cells is a powerful method for identifying the genes underlying cell biological functions and for annotating the fly genome. Here we describe the development of living-cell microarrays for screening large collections of RNAi-inducing double-stranded RNAs (dsRNAs) in *Drosophila* cells. The features of the microarrays consist of clusters of cells 200 μm in diameter, each with an RNAi-mediated depletion of a specific gene product. Because of the small size of the features, thousands of distinct dsRNAs can be screened on a single chip. The microarrays are suitable for quantitative and high-content cellular phenotyping and, in combination screens, for the identification of genetic suppressors, enhancers and synthetic lethal interactions. We used a prototype cell microarray with 384 different dsRNAs to identify previously unknown genes that affect cell proliferation and morphology, and, in a combination screen, that regulate dAkt/dPKB phosphorylation in the absence of dPTEN expression.

Despite the utility of RNAi for reducing gene function in mammalian systems, there are currently many benefits to carrying out genome-scale RNAi-mediated loss-of-function screening in *Drosophila* cells. First, in these cells RNAi induced by long double-stranded RNAs (dsRNAs) is highly effective[1], ensuring that the expression of the vast majority of target genes is reduced to a significant degree. Second, several genome-scale collections of dsRNAs are available[2–5], making it possible to undertake the systematic identification of genes that perform a given cell biological function. Third, in *Drosophila* cells two distinct dsRNAs can be used together to effectively silence two genes at the same time, enabling powerful combinations of loss-of-function screens for epistasis analysis and the identification of synthetic genetic relationships. Fourth, *Drosophila* has proven to be a good model organism for studying mammalian biological processes and diseases, with the added advantage of having a less redundant genome than do mammals.

To create a platform for genome-scale loss-of-function screening that is accessible to many researchers, we used the concepts underlying the cell microarray technology that we developed for mammalian cells[6] to create arrays of clusters of *Drosophila* cells, each with an RNAi-mediated reduction in the expression of a particular gene product. The method used to produce these *Drosophila* 'RNAi living-cell microarrays' is considerably different from the reverse transfection method we originally developed[6] and the methods based on reverse transfection that others[7–10] have used to transfect microarrayed siRNAs into mammalian cells. The particular properties of *Drosophila* cells required us to exploit new slide chemistries and develop new printing solutions and cell culture conditions. In sum, we have created a new, powerful dsRNA delivery platform for *Drosophila* cells that we anticipate will be the basis for the first robust genome-scale RNAi-based screens undertaken with living-cell microarray technology.

RESULTS

Development of RNAi living-cell microarrays

To make the microarrays, we print 2–3 nl of solutions of RNAi-inducing dsRNAs on a coated glass slide, plate *Drosophila* tissue culture cells on the arrays and incubate them for 3–4 d (**Fig. 1a**). The cells that settle on the 200-μm-diameter spots take up the dsRNAs that induce, through RNAi, the degradation of the targeted mRNAs and a concomitant decrease in the encoded proteins. *Drosophila* tissue culture cells do not adhere well to the polylysine- or γ-aminopropyl silane (GAPS)-coated surfaces we have used in mammalian cell microarrays, and thus we tested and found alternative slide surfaces that are compatible with *Drosophila* cells. In particular, we found that *Drosophila* cells stick and grow well on slides coated with amino non-silane or concanavalin A. To demonstrate our method, we printed arrays with dsRNAs that target GFP (green fluorescent protein; a control), DIAP1 (*Drosophila* inhibitor of apoptosis)[11,12] and dPTEN (the *Drosophila* homolog of the human PTEN tumor suppressor that represses the PI3K/Akt pathway)[13–15]. We then plated onto separate arrays Kc$_{167}$ (ref. 16) or S2R$^+$ (ref. 17) cells and, after 3 d in culture, processed the arrays for fluorescence microscopy. A nuclear stain (Hoechst 33342) revealed an absence of cells on the DIAP1 dsRNA spots, which is consistent with the known antiapoptotic role of the protein. The dPTEN dsRNA spots had greatly elevated levels of phosphorylated dAkt (**Fig. 1b**), the expected effect of reducing dPTEN expression. The cells on the control GFP dsRNA spots were indistinguishable from those on the nonprinted areas of the array (**Fig. 1b**). Consistent with the great potency of dsRNAs for
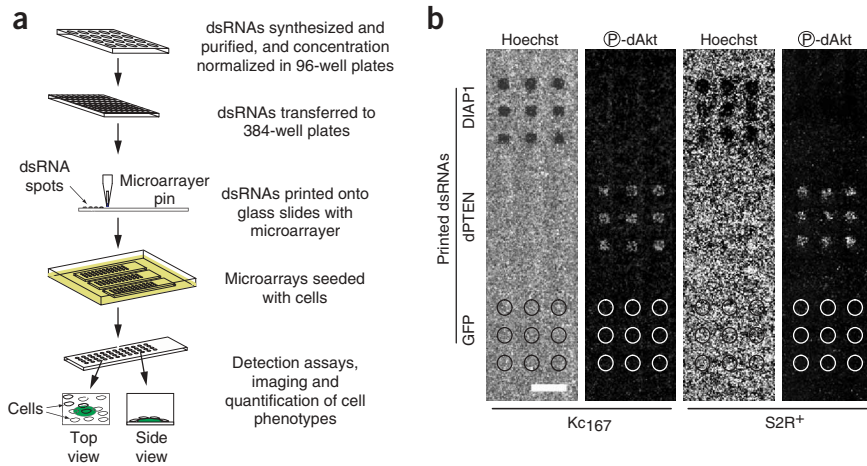
Figure 1 | *Drosophila* RNAi cell microarrays. (**a**) Schematic of procedure for the fabrication, cell seeding and assaying of *Drosophila* RNAi cell microarrays. (**b**) Low-magnification fluorescence images of Kc167 and S2R+ *Drosophila* cells cultured for 3 d on an array printed with dsRNA targeting GFP, DIAP1 and dPTEN and stained for nuclei (Hoechst 33342) and phospho-dAkt. Images reveal an absence of cells on the DIAP1 dsRNA spots and an increase in phospho-dAkt in cells on the dPTEN dsRNA spots. GFP dsRNA spots are indistinguishable from areas between dsRNA spots. Scale bar, 800 μm.

inducing RNAi in *Drosophila*, the method works well with dsRNAs printed over a wide range of concentrations (**Supplementary Fig. 1**).

## Combination loss-of-function screening with microarrays

To determine whether the arrays are compatible with combination screening of two different dsRNAs simultaneously, we printed an array with dsRNAs targeting GFP, the caspase DRONC[18] and dPTEN. Each was printed at three concentrations in quadruplicate. We seeded Kc167 cells on the array and cultured them to allow dsRNA uptake and a reduction in the expression of the targeted proteins. After 2 d in culture, we used a conventional soaking method[1] to transfect a dsRNA that targets DIAP1 into all the cells on the array—that is, cells growing both on and around the printed dsRNA spots. Depletion of DIAP1 causes massive cell death[12], as we had previously verified (**Fig. 1b**). Two days after adding the DIAP1 dsRNA, we exposed the cells to Sytox, a fluorescent molecule that stains only the nuclei of dead cells, and, after fixation, to Hoechst 33342, a dye that stains nuclei irrespective of cell viability. The arrays were then imaged with automated fluorescence microscopy (**Fig. 2a,b**) and the cells growing on the dsRNA spots analyzed with custom image analysis software (**Fig. 2c**). No cell clusters were apparent on the GFP dsRNA spots and they were indistinguishable from nonprinted areas of the array (**Fig. 2a**, top panels). Moreover, at both low (**Fig. 2a**) and high magnification (**Fig. 2b**), all the cells on the GFP dsRNA spots were Sytox positive, indicating that, as

expected, DIAP1 depletion killed the cells. In contrast, Hoechst-positive cell clusters grew on the spots printed with dsRNAs targeting DRONC or dPTEN (middle and bottom panels in **Fig. 2a**) and these spots contained about 4–5 times as many cells in total as the GFP dsRNA spots (**Fig. 2c**). At either low (**Fig. 2a**) or high magnification (**Fig. 2b**), no Sytox-positive cells were detected on the DRONC dsRNA printed spots, which is consistent with the essential role of DRONC in mediating cell death induced by DIAP1 depletion[12]. In contrast, most of the cells in the cell clusters on the dPTEN dsRNA spots were Sytox positive, indicating that they were dead (**Fig. 2a,b**). This suggests that the activation of the dPI3K/dAkt pathway induced by dPTEN loss delayed death long enough for the cells to divide and form clusters, but did not completely prevent cell death, a finding consistent with the known regulatory but nonessential role of PTEN in apoptosis[15]. Notably, this experiment also indicated that we can detect dose-response relationships on the arrays. As we lowered the concentration of the DRONC dsRNA in the spots, the cell number remained stable but the intensity of the Sytox staining increased, so that cell survivorship (nuclear count/Sytox intensity) decreased (**Fig. 2c**). It is likely that at the lower DRONC dsRNA concentrations, sufficient DRONC protein accumulates so that DIAP1-depletion can slowly trigger cell death and the increase in Sytox staining. We also demonstrated that two dsRNAs can be tested in combination by printing a mixture of both in one spot (**Supplementary Fig. 2**). The potentially unequal

Figure 2 | Epistasis analysis with a *Drosophila* RNAi cell microarray. (**a**) Kc167 cells were seeded onto an array printed in quadruplicate with dsRNAs at the indicated concentrations targeting GFP, the DRONC caspase or dPTEN. At 48 h after seeding, a dsRNA targeting DIAP1 was introduced into all cells on the array by the soaking method. After a further 48 h in culture, low-magnification images of the array were taken after staining for nuclei with Hoechst 33342 (blue) and dead cells with Sytox (green) staining. Scale bar, 800 μm. (**b**) High-magnification images from cells on indicated dsRNA spots from **a**. Scale bar, 20 μm. (**c**) Quantification of number of nuclei (top), Sytox intensity (middle) and survivorship (number of nuclei/Sytox intensity; bottom) of cells growing on dsRNA spots in **a**. Error bars, s.d. for n = 4.
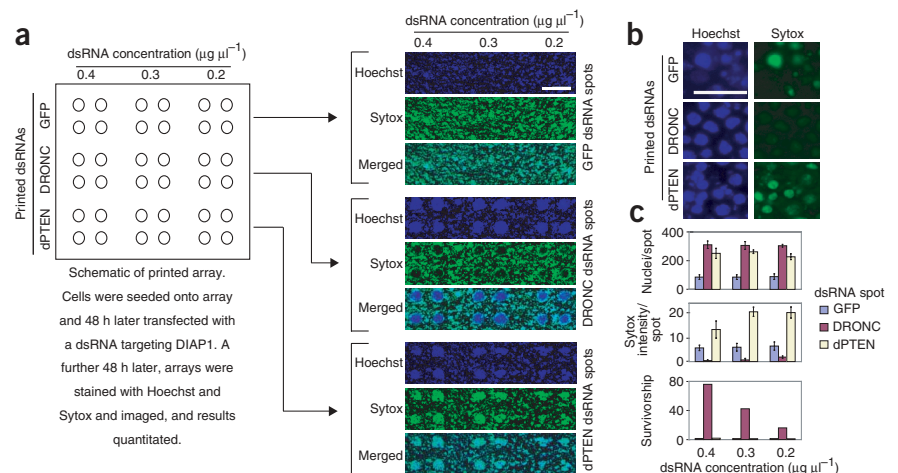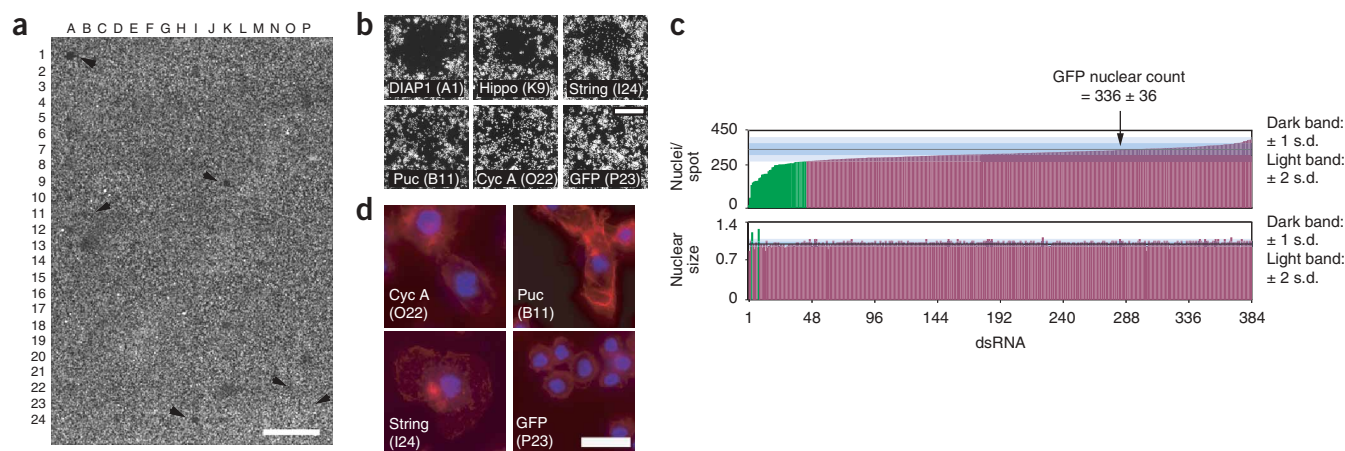
Figure 3 | Use of high-density RNAi cell microarrays to screen for regulators of cell number. (**a**) Bird's-eye view image of a nuclear stain of Kc_{167} cells cultured for 3 d on an array printed with 384 different dsRNAs. Arrows indicate spots shown in higher magnification in **b**, and several point to spots with low cell density. Scale bar, 2 mm. (**b**) Higher-magnification image of nuclear stain of dsRNA spots indicated with arrows in **a**. Scale bar, 200 μm. (**c**) Quantitative analysis of number of nuclei (top) and average nuclear size (bottom) of cells in dsRNA spots from **a**. Bar heights represent the number of nuclei or average nuclear size of cells in a dsRNA spot. Bars are arranged from left to right in order of increasing number of nuclei on the dsRNA spot. Green bars depict spots where the number of nuclei or the average nuclear size vary by at least 2 s.d. from the mean of control GFP dsRNA spots (indicated with an arrow). (**d**) Images capturing high content phenotypes of cells in spots with the indicated coordinates. Cells were stained for nuclei (blue) and actin (red). Scale bar, 20 μm.

half-lives of proteins need to be kept in mind, however, when searching for synthetic effects with co-printed dsRNAs.
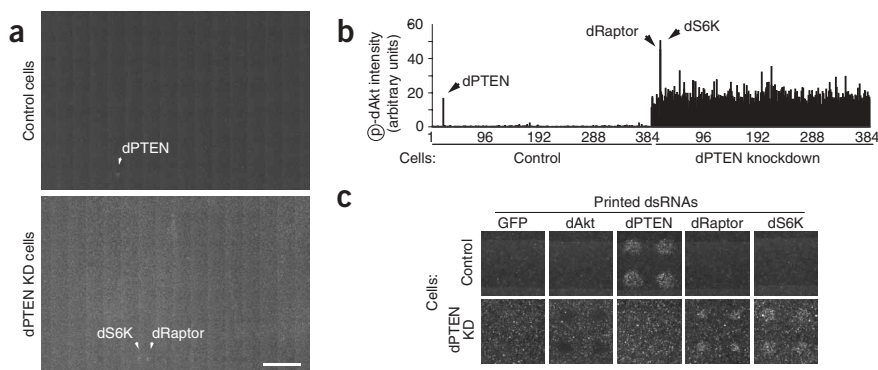
Quantitative screens using microarrays

To demonstrate the potential of the microarrays for unbiased high-throughput discovery screening, we printed arrays with 384 dsRNAs at a feature density that is compatible with the inclusion of at least 5,600 distinct dsRNAs on one glass slide of standard size. The genes targeted in the array include the majority of the tyrosine kinases annotated in the fly genome (41 of about 43), all predicted serine/threonine protein phosphatases and a varied assortment of other genes for which we had dsRNAs available (see **Supplementary Table 1** for a complete list). To screen for dsRNAs that affect cell number, we plated Kc_{167} cells on the array and after 3 d stained for nuclei and actin. We then imaged the array with automated microscopy and quantified the number and size of nuclei on each dsRNA spot. On a low-magnification image of the Hoechst-stained 384-element array, it is possible to detect tiny holes of low nuclear

Table 1 | Characteristics of the 44 genes targeted by dsRNAs printed in the spots from **Figure 3c** with significantly lower numbers of nuclei

Gene name	CG number	Nuclear count	Nuclear size	Gene name	CG number	Nuclear count	Nuclear size
DIAP1	CG12284	6	0.850	–	CG1542	242	1.001
Hippo	CG11228	51	1.048	–	CG10648	245	0.946
String	CG1395	126	1.179	l(1)G0334	CG7010	245	0.987
PP2A like	CG4733	140	0.986	Acyl CoA DH	CG9006	246	0.953
RpS6	CG10944	145	0.887	–	CG3983	246	0.964
Hoip	CG3949	149	0.995	Pp2B-14D	CG9842	246	0.911
desat1	CG5887	150	0.907	mts	CG7109	249	0.910
Cyclin A	CG5940	150	1.239	EGFR	CG10079	249	0.933
Pp1-96A	CG6593	166	0.963	Arc42	CG4703	250	0.982
Pvr	CG8222	170	0.968	–	CG14210	251	0.967
Pp1-13C	CG9156	186	0.898	B4	CG9239	253	0.976
Inr	CG18402	188	0.984	EP2237	CG4427	253	0.984
Pp1-87B	CG5650	191	0.857	Pp2A-29B	CG13383	254	0.935
Puckered	CG7850	191	1.049	l(2)08717	CG15095	258	0.959
PPV	CG12217	191	0.925	Bystin	CG1430	260	1.002
FAS	CG3523	206	0.948	Rheb	CG1081	260	0.999
–	CG14543	213	0.962	CanA-14F	CG9819	261	0.956
Flap wing	CG2096	215	0.910	MKP-like	CG7378	262	0.987
–	CG11451	229	0.974	Nopp140	CG7421	262	0.991
ACC	CG11198	231	0.990	–	CG6770	263	1.017
rad50	CG6339	241	1.009	Ddr	CG9490	264	1.021
Hsp83	CG1242	242	0.959	GFP	–	336	1.000

Figure 4 | Use of high-density RNAi cell microarrays for a quantitative screen for genes that regulate the phosphorylation of dAkt. (**a**) Bird's-eye view image of a phospho-dAkt immunofluorescence stain of Kc$_{167}$ cells cultured for 3 d on a duplicate array of one in **Figure 3a**. Cells were transfected with the GFP (control cells) or dPTEN (dPTEN KD cells) dsRNA 48 h before seeding on array. (**b**) Bar graphs showing levels of phospho-dAkt from spots on arrays shown in **a**. Bars are arranged from the A1 to the P24 position on the array. Many of the bars with low values are not visible in the highly dense graph shown, and bars for dS6K and dRaptor are next to each other and thus appear as one bar. (**c**) Confirmation on secondary arrays of the most prominent hits identified in **b**.

density (arrows in **Fig. 3a** point to spots shown in high magnification in **Fig. 3b**). These holes are quite obvious at a higher magnification (**Fig. 3b**) and correspond to spots printed with dsRNAs that target genes that are likely to be essential for normal cell proliferation, survival or adhesion to the slide.

The number of cells in 44 of the 384 spots on the array was at least two standard deviations below the mean number of cells on spots printed with a control dsRNA (**Fig. 3c**, green bars in top graph). Several of the dsRNAs printed in these spots target genes (**Table 1**) that are known to participate in cell cycle progression (cyclin A, string), apoptosis (DIAP1, Hippo), fatty acid synthesis (ACC, desat1, FAS) and protein synthesis (RpS6, Nopp-140). In addition, the list includes several genes without an annotated function (such as CG14210, CG14543 and CG6770). Many of the 44 dsRNAs that affect cell number target genes known to be cell essential, such as several protein phosphatases[19,20], or that one might expect to be (ribosomal protein S6, fatty acid synthase). In addition, 28 of the 44 genes were tested in a recent genome-scale RNAi screen[5] for genes that affect cell viability as measured with a cellular ATP assay. Of these 28 genes, 9 also affected cell viability (**Supplementary Table 2**). Despite the difference in screening assays, the majority of the genes having the greatest effects on cell number also have a role in cell viability[5]. Overlapping genes include named (Hoip, PVR, desat1, rpS6) and unknown (CG11451) genes.

Notably, in our cell number screen only the dsRNAs that target cyclin A and string significantly increased the mean size of the nuclei (**Fig. 3c**, bottom). This result is consistent with the known role of cyclin A and string in cell cycle progression through G2/M and the large cell–large nuclei phenotype visible in high-magnification images of the cells (**Fig. 3d**). The large nuclei visible may be caused by a G2/M arrest or endocycle DNA replication. In high-magnification images of other cell clusters with decreased cell number, we detected cells with abnormal actin cytoskeletons (such as Puckered, in spot B11 in **Fig. 3b,d**).

We next used the arrays to identify genes that, when knocked down, affect the phosphorylation state of dAkt in cells with or without dPTEN expression. With a traditional transfection

method, we introduced into duplicate cultures of Kc$_{167}$ cells a control (GFP) or a dPTEN dsRNA and then cultured the cells for 2 d to allow RNAi induction and dPTEN depletion. We plated these cells onto duplicate 384-element arrays and, after a further 3 d in culture, processed the arrays for Hoechst staining and phospho-dAkt immunofluorescence. We then imaged the arrays and quantified the level of the phospho-dAkt signal per cell using high-resolution images of each spot. On the array plated with the control cells, only the cells growing on the dPTEN dsRNA spot had visibly increased levels of phospho-dAkt (**Fig. 4a**, top, arrow), a result confirmed by quantitative image analysis of high-resolution images (**Fig. 4b**, left). On the array plated with the dPTEN knockdown cells, all the cells had a visibly (**Fig. 4a**) and quantifiably (**Fig. 4b**, right) higher basal level of phospho-dAkt. In addition, several dsRNAs increased phospho-dAkt levels above those caused by the dPTEN knockdown alone, whereas others suppressed phospho-dAkt levels (**Fig. 4b**; see **Supplementary Table 1** for all hits). On small arrays reprinted with the dsRNAs in quadruplicate, we confirmed the effects of the dsRNAs that caused the greatest increases and decreases in phospho-dAkt levels (**Fig. 4c**). Notably, the two dsRNAs that most increase phospho-dAkt levels target dS6K and dRaptor, which are both components of the target of rapamycin (TOR) pathway. The TOR pathway suppresses signaling by the PI3K pathway[21–23] and so knockdowns of raptor and S6K should activate Akt phosphorylation. Reassuringly, the dsRNA that most strongly suppressed phospho-dAkt levels targets dAkt itself, whereas others dsRNAs that decrease phospho-dAkt levels target genes not previously implicated in dAkt regulation (**Supplementary Table 1**).

DISCUSSION
In the era of whole-genome sequencing, an important goal is to understand the functions of each identified gene. The *Drosophila* RNAi living-cell microarrays described here allow traditional biological experiments to be conducted in living cells at an extremely high throughput: the entire fly genome can be analyzed using arrays contained on just three standard microscope slides. After staining, these slides can be analyzed at low resolution, analogous to an *in vivo* western blot, or at high resolution, which allows high content analysis of complex cellular phenotypes. The arrays can be used for genetic-like screens in *Drosophila* cells with the benefit that every gene is tested systematically and the genes corresponding to hits are easily identified. By reducing the expression of two genes simultaneously it is possible to discover synthetic genetic interactions, including suppression and enhancement. Application of the microarrays to systematically undertake synthetic interaction screens in *Drosophila* cells should prove a useful approach for revealing the structure and functions of signaling networks.

METHODS
dsRNA preparation. We amplified templates for dsRNA synthesis by RT-PCR (Qiagen) using total *Drosophila* S2 cell RNA and

gene-specific primers that incorporate the T7 promoter (5′-GAATTAATACGACTCACTATAGGGAGA-3′). We used Primer3 (http://frodo.wi.mit.edu/cgi-bin/primer3/primer3.cgi) to design primers based on cDNA sequences from FlyBase (www.flybase.org) and made the templates as long as possible, with a maximum size of 800 bp. We used 5 μl of template in a 20-μl *in vitro* transcription reaction mixture (MEGAscript, Ambion). After *in vitro* transcription reactions ran overnight at 37 °C, we added 2 U of DNase I (Ambion) to the reaction in 78 μl nuclease-free water (Ambion) and incubated it for 0.5 h at room temperature (24–26 °C). We then purified the dsRNA using 96-well PCR fragment vacuum purification plates (Millipore) and a vacuum manifold (Millipore) at 5 p.s.i. for 45 min. We eluted dsRNAs from the plates by adding 50 μl 10 mM Tris-Cl (pH 7.0) to the wells, sealing the plates and shaking them on a plate shaker for 20 min. After shaking, we added an additional 50 μl of 10 mM Tris-Cl (pH 7.0) to each well, mixed the samples by pipetting up and down five times, and transferred the dsRNA to storage plates (Costar). We determined dsRNA concentrations using a Nano-Drop spectrophotometer (NanoDrop Technologies) and stored samples at –20 °C until use.

Microarray printing. We used a commercially available robotic arrayer (PixSys 5500A; Cartesian Technologies) equipped with stealth pins (ArrayIt SMP7; Telechem) to print a dsRNA/salt solution from a 384-well titer plate (Greiner) onto either glass microscope slides (VWR) coated with 1 mg ml^{-1} concanavalin A (Sigma) in nuclease-free water or commercially made amino non-silane (DS8 chemistry) slides (Erie Scientific). Because of the potential variability of home-made concanavalin A slides, we currently use the commercial DS8 slides for all our arrays. SMP7 pins are reported to deposit 2.7 nl of sample with a spotting time of 25 ms. We printed arrays at room temperature and 55% relative humidity. The dsRNA/salt printing solution contained purified dsRNA at 0.05–0.6 μg μl^{-1} in 500 mM NaCl, 10 mM Tris buffer (pH 7.0) in a total volume of 20 μl. To provide reference points for automated microscopy, we printed 4 μM rhodamine B dye (Sigma) in 100 mg ml^{-1} poly-D,L-lactic acid (Polysciences) in methyl salicylate (Sigma) at a set distance from each corner of the array. We sealed printed slides in air-tight bags and stored them at −20 °C until use. Arrays have been stored for at least 60 d without any apparent deterioration in performance.

Cell culture and addition of cells to microarrays. We propagated *Drosophila* cell lines in full Schneider's medium (Schneider's *Drosophila* medium (Gibco) supplemented with 10% IFCS (in-activated fetal calf serum), 50 U ml^{-1} streptomycin and 0.05 mg ml^{-1} penicillin). We split Kc$_{167}$ cells once every 4 d and seeded them at 8×10^7 cells per 12 ml of fresh medium after each split. We split S2R$^+$ cells once every 4 d and seeded them at 1.5×10^7 cells per 12 ml of fresh medium. We 'seeded' arrays with cells prepared as follows. Cells that had been split ∼72 h previously and seeded at 8×10^7 cells in 12 ml medium in a T75 flask (Corning) were serum starved in their culture flasks in serum-free medium (Gibco) for 1 h. Cells were then harvested by scraping followed by pipetting up and down ten times with a 10-ml pipette, counted, pelleted and resuspended to 1.5×10^7 cells in 25 ml of fresh full Schneider's medium in a 50-ml tube. Before opening the airtight bags containing the arrays, we allowed the arrays at −20 °C to reach room temperature by leaving them for 1 h in a

tissue culture hood. We then placed, side by side, two printed slides and one dummy nonprinted slide in a 100 × 100 × 10–mm square tissue culture dishes (VWR). We poured the single-cell suspension from the 50-ml tube onto the dummy slide and allowed it to spread quickly over the printed slides. We then gently rocked the dishes back and forth twice to disperse the cells and placed them into a humidified 25 °C incubator. We incubated the arrays with cells for 68–96 h and then fixed them for 20 min at room temperature in PBS$^+$ (phosphate-buffered saline, 1 mM CaCl$_2$, 1 mM MgCl$_2$) containing 3.7% paraformaldehyde and 4.0% sucrose. For the synthetic DIAP1 experiments, we transfected cells that had been growing on the arrays for 48 h with the DIAP1 dsRNA by incubating them with 25 μg of the dsRNA in 25 ml of serum-free medium for 1 h, and then supplemented the medium to 10% IFCS. After a further 48 h incubation, we fixed the cells as above. For synthetic dPTEN experiments, we transfected 2.0×10^7 cells in 25 ml medium in a 10-cm-diameter round tissue culture dish with 50 μg of dPTEN dsRNA using Fugene (Roche), cultured the cells for 48 h and then added them to arrays as above.

Immunofluorescence and actin and DNA staining. All rinses and preparations were performed in PBS$^+$. If we performed DNA staining without immunofluorescence, we did not permeabilize the cells on the arrays. Slides were stored at 4 °C until imaging. For Sytox staining we incubated the cells with 0.5 μM Sytox in culture medium for 10 min before fixation. We fixed the arrays as above, permeabilized the cells with 0.1% Triton X-100 for 30 min and then probed with primary and secondary antibodies as previously described[6]. Incubation with the phospho-dAkt antibody was done overnight at 4 °C with a 1:500 dilution of primary rabbit polyclonal antibody specific for dAkt phosphorylated at Ser505 (Cell Signaling). We used a Cy3-labeled anti-rabbit secondary antibody from goats (Jackson Immunoresearch) at 2.5 μg ml^{-1} and incubated the mixtures at room temperature in the dark for 40 min. For F-actin staining, we added fluorescein-conjugated phalloidin (Molecular Probes) to the secondary antibody mix at 1.2 U ml^{-1}. This solution was then aspirated and the slides rinsed with PBS$^+$ and incubated in a Coplin jar containing 50 ml of 1 μg ml^{-1} Hoechst 33342 dye (Molecular Probes) in PBS$^+$ for 20 min to stain the DNA. We then rinsed the slides again and mounted them with Vectashield mounting medium (Vector Laboratories) and 26 × 60–mm cover glasses (VWR). We sealed the cover glasses onto the arrays with shiny top-coat nail polish (Sally Hansen).

Image acquisition and analysis. We acquired all images using an automated fluorescence microscope (Axiovert 200M, Zeiss) with custom image-acquisition software routines developed within the KS400 3.0 (Zeiss) platform. To quantify high-resolution images, we used CellProfiler, a custom image-analysis package that will be described elsewhere and made available to the academic community (www.cellprofiler.org). In brief, nucleus count and nuclear area are measured automatically by identifying nuclei based on local intensity maxima followed by water shedding. Intensity measurements are the integrated pixel intensities across the entire image, which is completely contained within a spot. All analysis was performed on images of a size of 200 × 200–μm centered on a cell cluster and captured with the 40× objective of the automated microscope.

Detailed protocols for all aspects of microarray construction and use are available as **Supplementary Methods** and also at http://jura.wi.mit.edu/sabatini_public/fly_array/index.htm.

Note: Supplementary information is available on the Nature Methods website.

COMPETING INTERESTS STATEMENT
The authors declare that they have no competing financial interests.

1. Clemens, J.C. *et al.* Use of double-stranded RNA interference in *Drosophila* cell lines to dissect signal transduction pathways. *Proc. Natl. Acad. Sci. USA* **97**, 6499–6503 (2000).
2. Lum, L. *et al.* Identification of Hedgehog pathway components by RNAi in *Drosophila* cultured cells. *Science* **299**, 2039–2045 (2003).
3. Kiger, A. *et al.* A functional genomic analysis of cell morphology using RNA interference. *J. Biol.* **2**, 27 (2003).
4. Foley, E. & O'Farrell, P.H. Functional dissection of an innate immune response by a genome-wide RNAi screen. *PLoS Biol.* **2**, E203 (2004).
5. Boutros, M. *et al.* Genome-wide RNAi analysis of growth and viability in *Drosophila* cells. *Science* **303**, 832–835 (2004).
6. Ziauddin, J. & Sabatini, D.M. Microarrays of cells expressing defined cDNAs. *Nature* **411**, 107–110 (2001).
7. Baghdoyan, S. *et al.* Quantitative analysis of highly parallel transfection in cell microarrays. *Nucleic Acids Res.* **32**, e77 (2004).
8. Mousses, S. *et al.* RNAi microarray analysis in cultured mammalian cells. *Genome Res.* **13**, 2341–2347 (2003).
9. Silva, J.M., Mizuno, H., Brady, A., Lucito, R. & Hannon, G.J. RNA interference microarrays: high-throughput loss-of-function genetics in mammalian cells. *Proc. Natl. Acad. Sci. USA* **101**, 6548–6552 (2004).
10. Yoshikawa, T. *et al.* Transfection microarray of human mesenchymal stem cells and on-chip siRNA gene knockdown. *J. Control. Release* **96**, 227–232 (2004).
11. Hay, B.A., Wassarman, D.A. & Rubin, G.M. *Drosophila* homologs of baculovirus inhibitor of apoptosis proteins function to block cell death. *Cell* **83**, 1253–1262 (1995).
12. Igaki, T., Yamamoto-Goto, Y., Tokushige, N., Kanda, H. & Miura, M. Down-regulation of DIAP1 triggers a novel *Drosophila* cell death pathway mediated by Dark and DRONC. *J. Biol. Chem.* **277**, 23103–23106 (2002).
13. Smith, A., Alrubaie, S., Coehlo, C., Leevers, S.J. & Ashworth, A. Alternative splicing of the *Drosophila* PTEN gene. *Biochim. Biophys. Acta* **1447**, 313–317 (1999).
14. Goberdhan, D.C., Paricio, N., Goodman, E.C., Mlodzik, M. & Wilson, C. *Drosophila* tumor suppressor PTEN controls cell size and number by antagonizing the Chico/PI3-kinase signaling pathway. *Genes Dev.* **13**, 3244–3258 (1999).
15. Huang, H. *et al.* PTEN affects cell size, cell proliferation and apoptosis during *Drosophila* eye development. *Development* **126**, 5365–5372 (1999).
16. Echalier, G. & Ohanessian, A. In vitro culture of *Drosophila* melanogaster embryonic cells. *In Vitro* **6**, 162–172 (1970).
17. Yanagawa, S., Lee, J.S. & Ishimoto, A. Identification and characterization of a novel line of *Drosophila* Schneider S2 cells that respond to wingless signaling. *J. Biol. Chem.* **273**, 32353–32359 (1998).
18. Dorstyn, L., Colussi, P.A., Quinn, L.M., Richardson, H. & Kumar, S. DRONC, an ecdysone-inducible *Drosophila* caspase. *Proc. Natl. Acad. Sci. USA* **96**, 4307–4312 (1999).
19. Li, X., Scuderi, A., Letsou, A. & Virshup, D.M. B56-associated protein phosphatase 2A is required for survival and protects from apoptosis in *Drosophila* melanogaster. *Mol. Cell. Biol.* **22**, 3674–3684 (2002).
20. Silverstein, A.M., Barrow, C.A., Davis, A.J. & Mumby, M.C. Actions of PP2A on the MAP kinase pathway and apoptosis are mediated by distinct regulatory subunits. *Proc. Natl. Acad. Sci. USA* **99**, 4221–4226 (2002).
21. Haruta, T. *et al.* A rapamycin-sensitive pathway down-regulates insulin signaling via phosphorylation and proteasomal degradation of insulin receptor substrate-1. *Mol. Endocrinol.* **14**, 783–794 (2000).
22. Radimerski, T., Montagne, J., Hemmings-Mieszczak, M. & Thomas, G. Lethality of *Drosophila* lacking TSC tumor suppressor function rescued by reducing dS6K signaling. *Genes Dev.* **16**, 2627–2632 (2002).
23. Radimerski, T. *et al.* dS6K-regulated cell growth is dPKB/dPI(3)K-independent, but requires dPDK1. *Nat. Cell Biol.* **4**, 251–255 (2002).